Received: 10 November 2022 | Revised: 12 November 2022 | Accepted: 12 November 2022

DOI: 10.1002/qre.3242

RESEARCH ARTICLE

WILEY

Another objection to the homogeneously weighted moving average control chart

Sven Knoth

Helmut Schmidt University, Hamburg, Germany

Correspondence
Sven Knoth, Department of Mathematics and Statistics, Helmut Schmidt University Hamburg, Holstenhofweg 85, 22043 Hamburg, Germany.
Email: knoth@hsu-hh.de

Abstract

It was recently demonstrated that homogeneously weighted moving average (HWMA) control charts are improper devices for an online detection of changes within a series of random variables. However, another attempt was made to bail out the concept underlying these charts. Here we want to re-emphasize that HWMA charts are dispensable by rebutting the arguments of the latter contribution.

KEYWORDS

average run-length, conditional detection delay, control chart, statistical process monitoring

1 | INTRODUCTION

During the last decade, many new procedures were introduced to the field of statistical process monitoring/control (SPM/C), where a substantial part should not be used in practice, as was discussed in Knoth et al. (2021, 2022).[1–3] Less surprisingly, attempts were started to regain reputation for the affected devices. In particular, Riaz et al. (2022)[4] provided new results for homogeneously weighted moving average (HWMA) control charts. The chart was introduced in Abbas (2018)[5] and became quite popular within a few years only. Knoth et al. (2021)[1] depicted the weaknesses of the HWMA chart by investigating the detection behavior for later changes. The authors deployed the conditional expected delay (CED) as function of the potential change point position. The change point marks the first observation subjected to a change (mostly in the mean). The CED profiles of the HWMA chart exhibit two remarkable patterns. After strikingly low values for very early changes (within the first few observations), the CED increases substantially granting the HWMA chart spoor detection performance for most of the interesting (potential) change point positions. Now, Riaz et al. (2022)[4] argued that the HWMA chart is superior not only for initial change points, which is usually shown by low zero-state average run-length (ARL) values. Recall that the zero-state ARL is a popular characteristic for measuring control chart performance introduced by Page.[6] But it is blind for any later change point position. For dealing with this situation, Riaz et al. (2022)[4] considered the limit of the CED, the well-known conditional steady-state ARL.[7] Their analysis, however, is imperfect for two reasons. First, their Monte Carlo study for calculating the CED is flawed. Second, the CED shape of the HWMA chart differs radically from all other considered control charts. In particular, the CED limit (i. e. the conditional steady-state ARL) is rather meaningless, because the convergence kicks in much too late. Riaz et al. (2022)[4] investigated change point positions beyond 10,000 (and much larger), which is huge compared to the chosen in-control ARL, namely 500.

In the next section, all the technical details such as the definition of the HWMA chart and of its competitor, the exponentially weighted moving average (EWMA) chart, are provided. In addition, all the performance measures are formally

defined. In Section 3, the HWMA versus EWMA comparison following Riaz et al. (2022)[4] is done, which illustrates the aforementioned weaknesses of the HWMA chart. Finally, conclusions are given in Section 4.

2 | THE HWMA CHART, THE EWMA CHART, AND PERFORMANCE MEASURES

2.1 | Preliminaries, models, and measures

For the sake of simplicity, let us consider a series of independent normally distributed $X_1, X_2, ...$ with mean μ and standard deviation $\sigma = 1$ (because we assume known standard deviation). Then we deploy the simple change point (τ) model

$$\mu = \begin{cases} \mu_0 = 0, & t < \tau \\ \mu_1 = \delta, & t \geq \tau \end{cases}. \tag{1}$$

The aim of any control chart (SPM tool) is to detect as quickly as possible that the current time index t fulfills $t \geq \tau$ with τ being unknown. Aside from that, false alarms should be avoided as much as possible. For signaling, we use the observations $X_1, X_2, \dots, X_t, \dots$ and compact them appropriately to elicit information about a potential change. With L, we label the index (in $\{1, 2, ...\}$), where the applied control chart declares that the change took place. Moreover, with $E_\tau()$, we denote the expectation for a given change point position τ. With this notation, we write the zero-state ARL as $E_\infty(L)$ and $E_1(L)$ for two specific cases, namely no change at all (in-control) or instant change, respectively. For all other cases, $1 < \tau < \infty$, we consider the CED

$$D_\tau = E_\tau(L - \tau + 1 \mid L \geq \tau) \tag{2}$$

and, if appropriate, its limit the conditional steady-state ARL

$$D_\infty = \lim_{\tau \to \infty} D_\tau \,. \tag{3}$$

2.2 | The HWMA chart

It was proposed by Abbas[5] and is calculated in the following way:

$$H_1 = \omega X_1 + (1 - \omega)\mu_0 \quad , H_t = \omega X_t + \frac{1 - \omega}{t - 1} \sum_{i=1}^{t-1} X_i \tag{4}$$

for $t = 2, 3, ...$, with $0 < \omega < 1$. Utilizing mean and standard deviation of H_t, the alarm rule L_H is derived as follows:

$$E_\infty(H_t) = \mu_0 \quad , Var(H_1) = \omega^2 \quad , Var(H_t) = \omega^2 + (1 - \omega)^2/(t - 1) \quad , \sigma_{H,t} := \sqrt{Var(H_t)},$$

$$L_H = \min\left\{t \geq 1 : |H_t - \mu_0| > c_H \sigma_{H,t}\right\}. \tag{5}$$

2.3 | The EWMA chart

Roberts[8] introduced the EWMA chart already more than 60 years ago. Here, we take advantage of the so-called exact control limits similarly to the aforementioned setup of the HWMA chart. Already MacGregor and Harris[9] reported that these limits equip the EWMA chart with some fast initial response features. It goes like

$$Z_0 = \mu_0 \quad , Z_t = (1 - \lambda)Z_{t-1} + \lambda X_t \quad , t = 1, 2, \dots ,$$

$$L_E = \min\left\{ t \geq 1 : |Z_t - \mu_0| > c_E \sigma_0 \sqrt{(1 - (1 - \lambda)^{2t}) \frac{\lambda}{2 - \lambda}} \right\}. \tag{6}$$

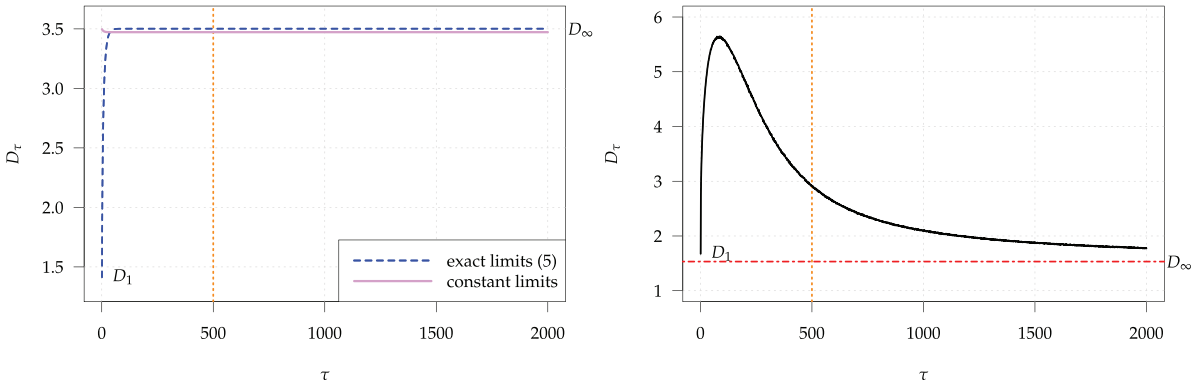

FIGURE 1 Exemplary CED analysis for control charts with head-start features, shift $\delta = 3$, EWMA with R package `spc` and HWMA with Monte Carlo (10^5 replicates)

Differently to the HMWA chart, various numerical routines are known to calculate the zero-state ARL, the CED, and the steady-state ARL. Here we make use of the implementations in the R package `spc`.[10] Note that we compare in this contribution HWMA charts and EWMA charts with $\omega = \lambda$ only.

3 | CED COMPARISON OF HWMA AND EWMA

3.1 | A further prelude

Utilizing the zero-state and conditional steady-state ARL, namely D_1 and D_∞, respectively, in Equation (2), implies some more or less hidden assumptions. For cumulative sum (CUSUM)[6,11] charts without head-start and EWMA charts with constant control limits (i. e., in Equation (6) one uses the asymptotic variance of Z_t and so the $1 - (1 - \lambda)^{2t}$ is replaced by its limit 1), $D_1 \geq D_\tau$ holds for all τ. Thus in this case, D_1 is some overall out-of-control measure. For the latter EWMA, the distance between D_1 and D_∞ is so small that it is sufficient to report D_1 anyway, compare to Knoth (2021)[7] for more details. For an illustration, see the corresponding CED curve in Figure 1 labeled by "constant limits." If one considers, however, control charts with head-start features like HWMA and EWMA chart with limits (5) and Equation (6), respectively, then D_1 could not be used alone to evaluate the detection performance. To illustrate this phenomenon, we consider EWMA ($\lambda = 0.05$) and HWMA ($\omega = 0.05$) with an in-control ARL of 500. In Figure 1, we present D_τ for $\tau = 1, 2, \ldots, 2000$.

In case of the EWMA chart, it is straightforward to accept that the pair (D_1, D_∞) sufficiently well characterizes the detection performance for the considered shift $\delta = 3$. The CED profile of the HWMA chart, however, exhibits a substantially different shape. For $\tau = 1, 2, \ldots, 50$, the CED as function of τ increases considerably and reaches somewhere between 50 and 100 its maximum (that is roughly equal to $5.6 > 3.5$, which is both D_∞ and $\sup_\tau D_\tau$ of the EWMA chart). Interestingly, all D_τ for $\tau = 60, 61, \ldots, 110$ are close to this maximum. For later change point positions $\tau \gg 100$, the CED D_τ starts decreasing in τ. Eventually, it converges to a really small value. It is not too complicated to calculate this limit. For $t \to \infty$, the HWMA term $1/(t-1)\sum X_i$ tends in the in-control case to $\mu_0 = 0$. This is valid both for the unconditional case (accidentally chosen in Riaz et al. (2022)[4]—see the discussion later) and in the conditional case of no false alarm. It is essentially a consequence of the law of large numbers. Moreover, the impact of any new out-of-control observation to the aforementioned sample average is negligible so that we can write:

$$H_t = \omega X_t + (1 - \omega)\mu_0 \quad \text{for } t \geq \tau \text{ and } \tau \text{ very large}\,.$$
$$|H_t - \mu_0| > c_H \sigma_{H,t} \quad \Leftrightarrow \quad |X_t - \mu_0| > c_H\,. \tag{7}$$

Thus, the HWMA chart behaves like a Shewhart chart, with control limit factor c_H, for very late observations. In the sequel, this limiting Shewhart chart will be denoted as the "distant Shewhart" chart.

For performing the comparison between the EWMA chart and the HWMA chart, we could either pick the mentioned $\sup_\tau D_\tau$, which was proposed already in Pollak and Siegmund,[12] as an omnibus delay measure, or we choose an appropriate range of interesting change point positions and do some qualitative comparison. In Knoth et al.,[1] the latter approach was

TABLE 1 Control limit factors for the EWMA and the HWMA charts for an in-control ARL 500, taken originally from Abbas[5]; the HWMA chart values c_H are checked by Monte Carlo (10^8 replications) results in the last row (standard error is between 0.037 and 0.050)

λ or ω	0.03	0.05	0.10	0.25	0.50	0.75
c_Z	2.483	2.639	2.824	3.001	3.072	3.088
c_H	2.272	2.608	2.938	3.075	3.089	3.090
$\widehat{E_\infty(L)}$	501.67	499.04	500.39	500.31	499.75	499.72

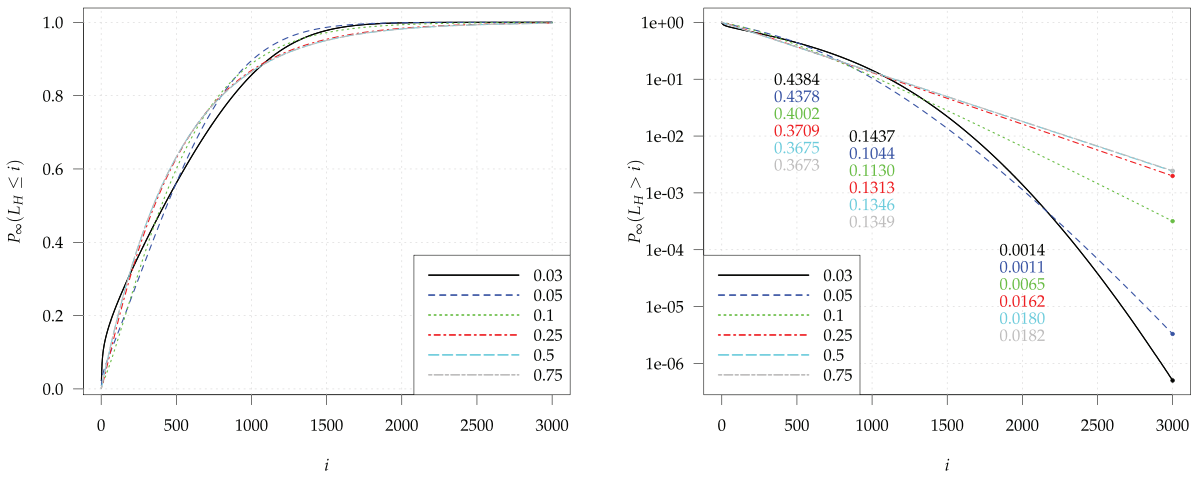

FIGURE 2 Run-length distribution in the in-control case; HWMA chart; Monte Carlo (10^{10} replicates); various ω (see legend)

utilized while considering $\tau \in \{1, 2, \dots, 500\}$. Riaz et al.[4] applied much wider ranges. For shifts δ smaller than 4, the upper bound was larger than 10,000 (in case of $\delta = 0.75$ for $\omega = 0.03$ it was even 100,000). The objective was presumably to enforce CED values close to the limit D_∞. For small δ, it converges quite slowly.

Regrettably, no explanation was given for looking at change point positions so much larger than the in-control ARL, 500, which was the upper bound in Knoth et al.[1] Here, we adopt this bound by investigating the in-control run-length distribution. For all considered HWMA configurations, see Table 1, we calculated the in-control run-length distribution in a large Monte Carlo study with 10^{10} replications. We need this large sample size because of the thin tails, for example, $P_\infty(L_H > 3\,000) < 10^{-6}$ for $\omega = 0.03$. In Figure 2, we plot the cumulative distribution function (cdf) $P_\infty(L_H \le i)$ and the survival function $P_\infty(L_H > i)$, both for $i = 1, 2, \dots, 3000$. The latter function is plotted on a log scale to allow a better judgment of the distribution tails.

Here we conclude that for small $\omega \in \{0.03, 0.05\}$, it is rather quirky to consider change point positions beyond 2000 because $P_\infty(L_H > 2\,000) < 0.002$. Going beyond 3000 is even more subtle, because these values fall below 0.000005. It is less pronounced for $\omega = 0.1$, of course. But even for larger $\omega \in \{0.25, 0.5, 0.75\}$, this probability is with $P_\infty(L > 2000) < 0.02$ small. Note that in this case, the distribution of L_H nearly coincides with the run-length distribution of the plain Shewhart chart with control limit factor $c_S = 3.0902$. This does not surprise, if we compare c_S with the values of c_H from Table 1 for $\omega \in \{0.25, 0.5, 0.75\}$: 3.075, 3.089, and 3.090. Thus, we choose $\{1, 2, \dots, 2\,000\}$ as set of interesting change point positions. Expanding it beyond 2000 is both futile and really cumbersome. To achieve an effective Monte Carlo sample size of, say, 10^5, one has to generate more than $5 \cdot 10^7$ runs for $\tau = 2\,000$ already ($\omega \in \{0.03, 0.05\}$), because many of the runs have to be dropped. Recall that we have to ensure the condition $L_H \ge \tau$. This is not a problem for common control charts, because much smaller values of τ are needed to get a stable result for the (conditional) steady-state ARL, compare to Taylor,[13] who used $\tau = 51$ for dealing with the CUSUM chart.

Riaz et al.[4] somehow confused the CED concept. From the description of the Monte Carlo design in a flowchart given as Figure 1,[4] one concludes that not the CED was determined. Instead, a run of length τ without applying the alarm rule (5) was produced. Subsequently, the resulting H_τ was used as "empirical" head-start to determine the actual run-length. The problem consists in the fact that these H_τ values are collected from the wrong distribution. Essentially, the following alarm rule was (implicitly) evaluated:

$$\tilde{L}_H = \min\left\{t \ge \tau + 1 : |H_t - \mu_0| > c_H \sigma_{H,t}\right\}. \tag{8}$$

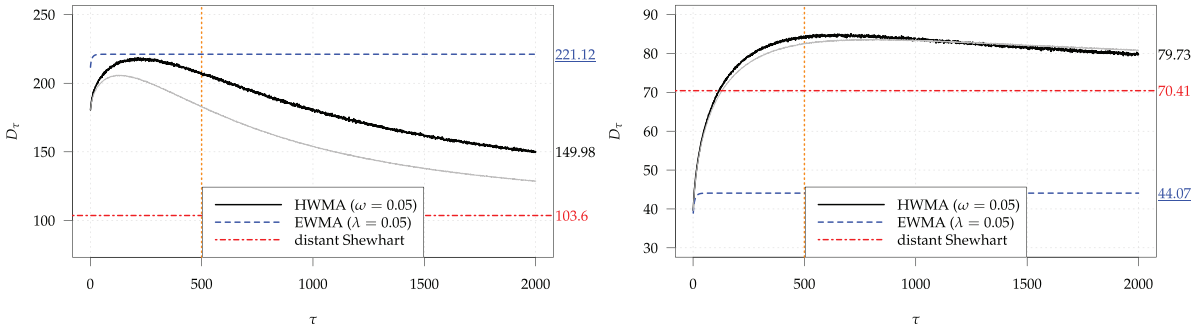

FIGURE 3 CED D_τ, $\omega = \lambda = 0.05$, HWMA with Monte Carlo with 10^6 (wrong D_τ, gray lines) and 10^5 replicates, EWMA chart with R package `spc`

Thus, Riaz et al.[4] estimated $E_\tau(\tilde{L}_H)$ instead of $D_\tau = E_\tau(L_H - \tau + 1 \mid L_H \geq \tau)$. In other words, the latter authors evaluated control chart designs, which run without activated alarm rule along the first τ observations. This quite unusual approach needs some justification. But it does not refer to the common CED concept anyway. The impact to the CED results could be severe (in particular for small ω), as we can see in the next section. On the other hand, this erroneous approach is tempting because no observations have to be dropped. Finally, it has to be noted that Riaz et al.[4] marked with τ the last in-control observation, whereas in our change point model in Equation (2), τ labels the first out-of-control one.

There is another problem with the HWMA chart for late time indices t. Both in-control cdf of the HWMA and the EWMA chart feature geometric tails. For all EWMA configurations, these tails correspond to Shewhart charts (exact geometric) with in-control ARL levels from *534* ($\lambda = 0.03$) to 500 ($\lambda = 0.75$). However, the tails for the HWMA chart relate to Shewhart charts with control limit c_H (see Table 1), resulting in in-control ARL levels of *77*, 121, and 211 for $\omega = 0.03, 0.05$, and *0.1*, respectively. Thus, long running HWMA charts become more and more sensitive to false alarms. This is different to common control charts. For $\omega = 0.25$ with an ARL of 372, it is less pronounced, but only for large $\omega \in \{0.5, 0.75\}$, the problem disappears. The problem remains also within the erroneous CED setup of Riaz et al.[4] Their CED analysis for huge τ ignores completely that the quick detection of very late ($\tau \gg 500$) change points is bought by a substantially increased false alarm rate.

3.2 | Actual comparison

For the sake of a concise presentation, we store the whole set of CED diagrams ($72 = 6 \times 12$ for $\omega \in \{0.03, \ldots, 0.75\}$ and $\delta \in \{0.125, \ldots, 5\}$) in the supplement. In order to summarize these many figures, we report the subset $\tau \in \{\tau_1, \ldots, \tau_2\}$ where D_τ is smaller for the EWMA chart than for the HWMA chart by providing the corresponding pairs (τ_1, τ_2) in Table 2. Moreover, we add superscripts *, **, *** and $^+$, $^{++}$, $^{+++}$ to mark the "vehemence" of the decision that the EWMA chart is better and worse, respectively, than the HWMA chart. With * and $^+$, we label the cases, where the majority of $\tau \in \{1, 2, \ldots, 2000\}$ refer to lower D_τ values of EWMA and HWMA, respectively. Then ** and $^{++}$ tag the cases where nearly all τ maintain these patterns. Eventually, *** and $^{+++}$ designate the instances, where it is valid for all $\tau = 1, 2, \ldots$. Before we discuss the results given in Table 2, we provide for all utilized annotations an example.

We start with the straightforward cases, namely *** and $^{+++}$. Interestingly, there are 12 instances of the EWMA chart being uniformly quicker (***), whereas only in one case the HWMA chart takes the lead ($^{+++}$). For the configuration $\omega = 0.05 = \lambda$, we observe *** for $\delta \in \{0.375, 0.5, 1, 1.5\}$ and $^{+++}$ for $\delta = 0.125$. In Figure 3, we look at $\delta = 0.125$ and *0.375*.

The true CED (black solid lines) results of the HWMA chart are calculated with 10^5 Monte Carlo replications, whereas the wrong ones (gray solid lines) from Equation (8) are obtained with 10^6 replicates. Note that the difference between these two curves is substantial for $\delta = 0.125$ (left-hand side in Figure 3). Both, the correct D_τ and the wrong $E_\tau(\tilde{L}_H)$ converge finally to the out-of-control ARL value of the "distant" Shewhart chart, that is, the conditional steady-state ARL of HWMA D_∞. It is easy to see from Figure 3 that for $\omega = 0.05$ and $\delta = 0.125$, the CED D_τ of the HWMA chart is smaller than the one of the EWMA chart for all τ. Similarly we conclude the reverse case for $\delta = 0.375$, where D_τ of the EWMA chart is uniformly smaller.

The rule for either *** and $^{+++}$ is quite simple—one of the designs beats the other for all τ. We apply a more involved mechanism for the other labels. Having in mind our definition that for $\tau_1 \leq \tau \leq \tau_2$, the CED D_τ of the EWMA chart is

TABLE 2 CED comparison results of HWMA and EWMA charts with $\omega = \lambda$; (τ_1, τ_2) labels the subset of $\{1, 2, \ldots, 2000\}$, where the EWMA chart exhibits smaller CED (D_τ) values than the HWMA chart; with *, **, ***, we mark the cases where the majority, nearly all and all τ, respectively, support the dominance of the EWMA chart, whereas $^{+}$, $^{++}$, $^{+++}$ does it for the superiority of the HWMA chart.

	δ											
ω	**0.125**	**0.25**	**0.375**	**0.5**	**0.75**	**1**	**1.5**	**2**	**2.5**	**3**	**4**	**5**
0.03	$(50,756)^{*}$	$(11,2000)^{**}$	$(6,2000)^{**}$	$(5,2000)^{**}$	$(4,2000)^{**}$	$(2,2000)^{**}$	$(1,2000)^{**}$	$(1,1217)^{**}$	$(1,782)^{*}$	$(1,551)^{*}$	$(1,313)^{+}$	$(2,200)^{+}$
0.05	$(NA,NA)^{+++}$	$(12,2000)^{**}$	$(1,2000)^{***}$	$(1,2000)^{***}$	$(1,2000)^{***}$	$(1,2000)^{***}$	$(1,2000)^{***}$	$(1,1425)^{**}$	$(1,611)^{*}$	$(1,372)^{+}$	$(1,185)^{+}$	$(2,112)^{+}$
0.10	$(1258,2000)^{++}$	$(57,2000)^{**}$	$(12,2000)^{**}$	$(2,2000)^{**}$	$(1,2000)^{***}$	$(1,2000)^{***}$	$(1,2000)^{***}$	$(1,2000)^{***}$	$(1,978)^{*}$	$(1,223)^{+}$	$(1,42)^{++}$	$(2,29)^{++}$
0.25	$(247,2000)^{*}$	$(94,2000)^{*}$	$(43,2000)^{**}$	$(20,2000)^{**}$	$(6,2000)^{**}$	$(3,2000)^{**}$	$(1,2000)^{***}$	$(1,2000)^{***}$	$(1,2000)^{***}$	$(1,247)^{+}$	$(1,15)^{++}$	$(2,9)^{++}$
0.50	$(91,2000)^{*}$	$(58,2000)^{*}$	$(33,2000)^{**}$	$(20,2000)^{**}$	$(9,2000)^{**}$	$(5,2000)^{**}$	$(2,2000)^{**}$	$(2,2000)^{**}$	$(2,2000)^{**}$	$(2,2000)^{**}$	$(1,5)^{++}$	$(1,4)^{++}$
0.75	$(16,2000)^{**}$	$(19,2000)^{**}$	$(15,2000)^{**}$	$(10,2000)^{**}$	$(6,2000)^{**}$	$(3,2000)^{**}$	$(2,2000)^{**}$	$(2,2000)^{**}$	$(2,2000)^{**}$	$(2,2000)^{**}$	$(1,4)^{++}$	$(2,2)^{++}$

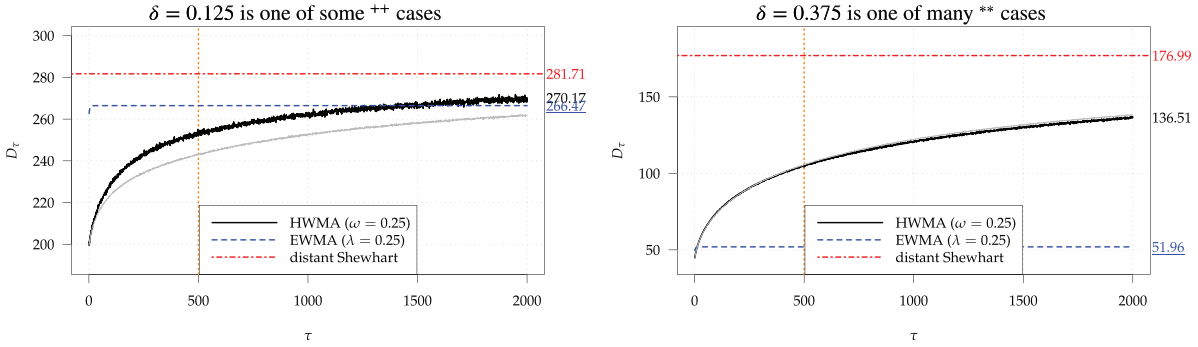

FIGURE 4 CED D_τ, $\omega = \lambda = 0.1$, HWMA with Monte Carlo with 10^6 (wrong D_τ, gray lines) and 10^5 replicates, EWMA chart with R package spc

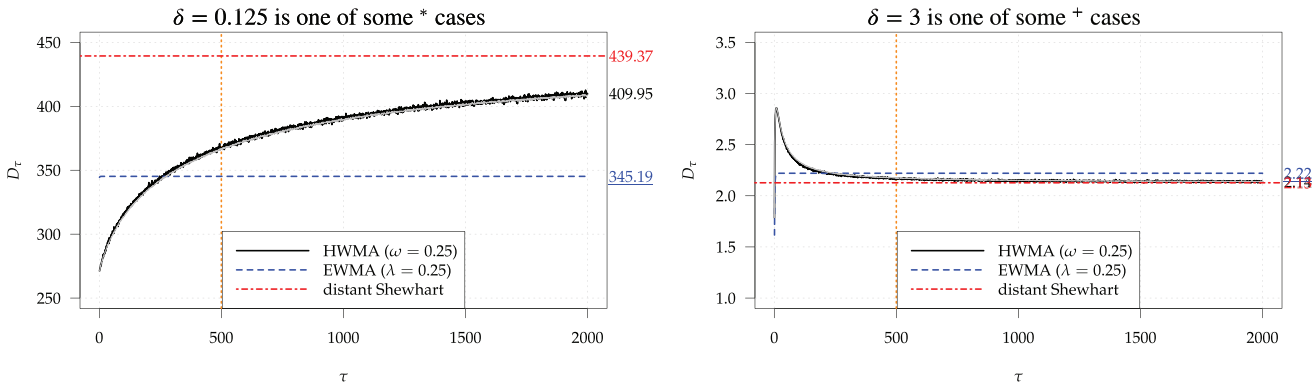

FIGURE 5 CED D_τ, $\omega = \lambda = 0.25$, HWMA with Monte Carlo with 10^6 (wrong D_τ, gray lines) and 10^5 replicates, EWMA chart with R package spc

smaller than the one of the HWMA chart, we look at $P_\infty(\tau_1 \le L_H \le \tau_2)$ for given ω and assign **, *, $^{+}$, and $^{++}$ if this probability is larger than 0.9, between 0.9 and 0.5, between 0.5 and 0.1, and smaller than 0.1, respectively. Thus it is more than just counting the τ, which would result simply in $\tau_2 - \tau_1 + 1$.

We continue with the nearly unique cases ** and $^{++}$ in Figure 4. For the configuration $\omega = 0.1 = \lambda$, we observe them for $\delta \in \{0.375, 0.5\}$ and $\delta \in \{0.125, 4, 5\}$, respectively. As for $\omega = 0.05$, we select the shifts $\delta = 0.125$ and 0.375 for display in Figure 4.

For $\delta = 0.375$ (i. e., the ** case), D_τ of the HWMA chart is smaller than of the EWMA chart only for a few values, $1 \le \tau \le 11$. Thus, it is "nearly" a *** case. There are ** cases, for example, $\delta = 0.25$, where it is more ambiguous because having the wider interval $1 \le \tau \le 56$. Turning to $\delta = 0.125$, we indicate that D_τ is smaller for the EWMA chart than for the HWMA chart for all $\tau \ge 1\,258$ including the limit D_∞. The latter is less impressive if we take into account that $P_\infty(L_H < 1\,258) = 0.944$. Thus, it is really a $^{++}$ case declaring that the HWMA chart performs better than the EWMA chart for this specific shift. In summary, the idea behind the formation of these ** and $^{++}$ cases is that there is nearly no doubt about the decision which control chart is better.

Next, we look at some * and $^{+}$ cases. In case of $\omega = 0.25$, we identify $\delta \in \{0.125, 0.25\}$ and $\delta = 3$ for * and $^{+}$, respectively. Picking $\delta = 0.125$ and *3*, we get to Figure 5. For both, one chart exhibits lower D_τ results for $1 \le \tau \le 247$, while the other one yields lower

numbers for $\tau > 247$. Because $P_\infty(L_H \le 247) = 0.377 < 0.5$, the chart with the better performance for $\tau > 247$ gives the superscript, * for $\delta = 0.125$ and $^{+}$ for $\delta = 3$.

Finally, two cases are discussed where the probability-based selection procedure returns rather vague results. Look at $(\omega = 0.03, \delta = 2.5)$ and $(\omega = 0.25, \delta = 0.25)$. Both are labeled as *. In Figure 6, the CED curves are provided.

For case $(\omega = 0.03, \delta = 2.5)$, Knoth et al.[1] would render a clear positive judgment for the EWMA chart, because for performing the CED comparison the smaller set $1 \le \tau \le 500$ was taken into account. Riaz et al.,[4] however, would declare that the HWMA chart is better because its D_∞ (distant Shewhart) is with *1.69* much smaller than the 4.85 of the opponent.

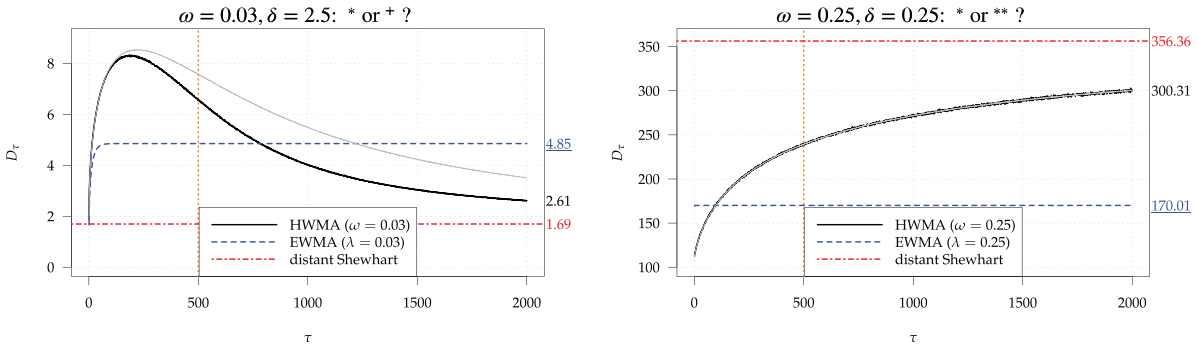

FIGURE 6 CED D_τ, HWMA with Monte Carlo with 10^6 (wrong D_τ, gray lines) and 10^5 replicates, EWMA chart with R package `spc`; limits of the decision procedure

From $P_\infty(1 \le L_H \le 782) = 0.748$ (at 783 the CED of the HWMA chart gets smaller than 4.85), we derived the tag *, that is, EWMA is slightly better. Because $(2\,000 - 782)/2\,000 \approx 0.61$, one might conclude that the HWMA chart is the better one. We believe that it is difficult to convince the SPM community or the ordinary practitioner that for an in-control ARL of *500*, it is more important to detect a change between observation 749 and 2000 than between 1 and 748. Utilizing $P_\infty(\tau_1 \le L_H \le \tau_2)$, as we did, is one way to avoid bewilderment. Turning to the other * case on the right-hand side of Figure 6, this probability acts reversely. This time, the HWMA chart features lower (than the EWMA chart) D_τ values at early positions, namely for $1 \le \tau \le 93$. A mechanical judgment of D_∞ would declare that the EWMA chart is the clear winner requesting the label **. However, after checking $P_\infty(94 \le L_H \le 2\,000) = 0.831$, we decide for the more "cautious" * label, because $0.831 \le 0.9$. It is not surprising that these decision procedures are not perfect. At least, we have only a few of these rather unclear cases.

After presenting the labeling procedure and discussing some examples, we will look at the *72* results collected in Table 2. By using the mentioned labels from $^{***}, ^{**}, \ldots$ to $^{+++}$, we conclude that for shifts $0.25 \le \delta \le 2.5$, the EWMA chart provides for all considered values of $\omega = \lambda$ the best CED performance. The HWMA chart does a good job only in case of very large changes, namely $\delta \in \{4, 5\}$, where it dominates for all ω. For the large change $\delta = 3$, the HWMA chart is better for $\omega \in \{0.05, 0.10, 0.25\}$, whereas the EWMA chart is better for the other three. A similar pattern could be observed for the smallest shift $\delta = 0.125$. Now the HWMA chart is the better one for $\omega \in \{0.10, 0.25\}$. In other words, the HWMA chart exhibits a decent CED performance only for very small changes ($\delta = 0.125$) and large changes ($\delta \ge 3$). A change of size $\delta = 0.125$ is mostly beyond the scope of a monitoring procedure. It is highly questionable, whether in SPM practice changes smaller than $\delta = 0.5$ are in focus. Typically, one has to estimate the parameters of the in-control model (here μ_0 and σ_0). Then a to be detected shift of size $\delta = 0.125$ is hidden in the estimation noise. For this very problem we refer to Woodall and Faltin.[14]

To consider the good performance of the HWMA chart for large changes, we provide some further details in Table 3. We present the steady-state ARL values, D_∞, of both charts for $\delta \in \{3, 4, 5\}$ augmented by the index, wherefrom the HWMA chart features lower values D_τ than the D_∞ of the EWMA chart. Recall that for the EWMA chart, D_∞ coincides with $\sup_\tau D_\tau$.

Starting with $\omega \in \{0.25, 0.5, 0.75\}$, we conclude that the differences in D_∞ between the HWMA chart and EWMA chart are so small that they would not influence the decision about what chart has to be applied. Turning to the smaller $\omega \in \{0.03, 0.05, 0.1\}$ we start with the most moderate shift, $\delta = 3$. The difference between *1.30* for the HWMA chart and *4.08* of the EWMA chart is substantial. But the sequence of D_τ for the HWMA chart remains above 4.08 for $1 \le \tau \le 551$, which weakens considerably this advantage. The same could be said for the other two values of ω. Eventually, we have the very large shifts $\delta \in \{4, 5\}$ with some advantage for the HWMA chart. Changes of this size, however, belong to the realm of the plain Shewhart chart (see the last row in Table 3). It is difficult to believe that because of $D_\infty = 1.04$ of the HWMA chart being smaller than $D_\infty = 3.14$ of the EWMA chart, one decides to utilize HWMA ($\omega = 0.03$) instead of EWMA ($\lambda = 0.03$). From Table 2, we know that for the $\omega = 0.03 = \lambda$ competition, the EWMA chart features better CED profiles for shifts $0.125 \le \delta \le 3$. Recall that we look for small ω (or λ), if we are interested in effective detection of small shifts. The odd behavior of the HWMA chart that D_∞ is monotone increasing in ω for all shifts δ creates all the confusion. This monotonicity is driven by the pattern that the control limit factor c_H in Equation (5) is increasing in ω (see Table 1). Together with the long run behavior ($t \to \infty$) of H_t, which acts then like a standard Shewhart chart with c_H as control limit, we obtain this pattern. Eventually, if these very large changes are so important, then one should use the

TABLE 3 Steady-state ARL, D_∞, of HWMA (H) and EWMA (e) charts with $\omega = \lambda$ for large shifts $\delta \in \{3, 4, 5\}$; index τ wherefrom D_τ of the HWMA chart is smaller than D_∞ of the EWMA chart is added as superscript (∞ marks the case that it is never smaller)

	δ			
ω	**3**	**4**	**5**	**Chart**
0.03	$1.30^{(552)}$	$1.04^{(314)}$	$1.02^{(201)}$	H
	4.08	3.14	2.59	e
0.05	$1.53^{(373)}$	$1.09^{(186)}$	$1.02^{(113)}$	H
	3.50	2.70	2.24	e
0.10	$1.91^{(224)}$	$1.19^{(43)}$	$1.02^{(30)}$	H
	2.86	2.20	1.83	e
0.25	$2.13^{(248)}$	$1.22^{(16)}$	$1.03^{(10)}$	H
	2.22	1.69	1.38	e
0.50	$2.15^{(\infty)}$	$1.22^{(6)}$	$1.03^{(5)}$	H
	1.91	1.36	1.10	e
0.75	$2.16^{(\infty)}$	$1.22^{(5)}$	$1.03^{(3)}$	H
	1.87	1.23	1.04	e
1	2.15	1.22	1.03	Shewhart

combined EMWA–Shewhart chart, where Capizzi and Masarotto[15] provide a reliable numerical algorithm for calculating the ARL.

4 | CONCLUSIONS

We demonstrated that for control charts like the HWMA chart, an analysis of the CED in Equation (2) is essential. Utilizing the zero-state and (conditional) steady-state ARL, D_1 and D_∞, respectively, alone is mostly misleading. For performing an appropriate CED analysis, the choice of the relevant change point positions is important. It is plausible to take the in-control ARL into account. In this paper, the zero-state in-control ARL was set to $E_\infty(L) = 500$ similarly to preceding contributions.[1,4] Thus, obvious choices for the upper bound of this set are 500, 1000, and 2000. Using larger values is inappropriate for two reasons. (i) The CED D_τ incorporates the conditioning on $L \geq \tau$. The probability $P_\infty(L_H > 2\,000)$ varies between *0.001* and 0.018 for the considered $\omega \in \{0.03, 0.05, \ldots, 0.75\}$. Thus, choosing $\tau > 2\,000$ implies that we condition on events which occur only very seldom. This is rather meaningless. If we would expand it to *3000* or even 5000, then we have to acknowledge the very low probabilities $P_\infty(L_H > 3000)$ and $P_\infty(L_H > 5\,000)$. For *3000*, we observe values between 0.002 and $5 \cdot 10^{-7}$, whereas for 5000, they are between $4 \cdot 10^{-6}$ and the machine epsilon of the used computer architecture, that is, roughly zero. (ii) Except for the limit D_∞, we have to use Monte Carlo studies to determine D_τ. The $L \geq \tau$ condition induces drops of runs, the lower the probability $P_\infty(L \geq \tau)$, the more runs are dropped. Thus, we would need a really huge number of Monte Carlo runs to achieve a decent estimation accuracy. This is not feasible anymore as soon as these probabilities fall below 10^{-5}.

Eventually, while assuming that the monitoring survived the first 2000 observations without false alarm, we arrive at time indices where the HWMA chart for $\omega \in \{0.03, 0.05, 0.1\}$ generates much more false alarms than all the competitors. Thus, comparing HWMA charts to other control charts by considering their D_τ values for very large τ is pointless.

For the given CED framework ($1 \leq \tau \leq 2000$), we found that the EWMA chart performs better for the majority of shifts, namely $\delta \in \{0.25, 0375, \ldots, 2.5\}$. There is no clear winner for shift $\delta = 3$. Only for very large shifts, $\delta \in \{4, 5\}$, the HWMA chart is more effective. We demonstrated that these advantages are not sufficiently substantial to change from the EWMA chart to the HWMA chart. Because EWMA charts are well-established, easier to setup and evaluate (keyword Markov property) and perform nearly always better, there is no reason to apply HWMA charts. Note the very simple setup of the comparison—we compared HWMA and EWMA charts with $\omega = \lambda$. Tuning λ will provide more advantages to EWMA.

DATA AVAILABILITY STATEMENT

Data sharing not applicable "no new data generated."

ORCID

Sven Knoth https://orcid.org/0000-0002-9666-5554

REFERENCES

1. Knoth S, Tercero-Gómez VG, Khakifirooz M, Woodall WH. The impracticality of homogeneously weighted moving average and progressive mean control chart approaches. *Qual Reliab Eng Int*. 2021;37(8):3779-3794. https://doi.org/10.1002/qre.2950
2. Knoth S, Woodall WH, Tercero-Gómez VG. The case against generally weighted moving average (GWMA) control charts. *Qual Eng*. 2022;34(1):75-81. https://doi.org/10.1080/08982112.2021.2002359
3. Knoth S, Saleh NA, Mahmoud MA, Woodall WH, Tercero-Gómez VG. A critique of a variety of "Memory-Based" process monitoring methods. *J Qual Technol*. 2022:1-27. https://doi.org/10.1080/00224065.2022.2034487
4. Riaz M, Ahmad S, Mahmood T, Abbas N. On reassessment of the HWMA chart for process monitoring. *Processes*. 2022;10(6):1129. https://doi.org/10.3390/pr10061129
5. Abbas N. Homogeneously weighted moving average control chart with an application in substrate manufacturing process. *Comput Ind Eng*. 2018;120:460-470. https://doi.org/10.1016/j.cie.2018.05.009
6. Page ES. Continuous inspection schemes. *Biometrika*. 1954;41(1-2):100-115. https://doi.org/10.1093/biomet/41.1-2.100
7. Knoth S. Steady-state average run length(s)—methodology, formulas and numerics. *Seq Anal*. 2021;40(3):405-426. https://doi.org/10.1080/07474946.2021.1940501
8. Roberts SW. Control chart tests based on geometric moving averages. *Technometrics*. 1959;1(3):239-250. https://doi.org/10.1080/00401706.1959.10489860
9. MacGregor JF, Harris TJ. Discussion of: exponentially weighted moving average control schemes: properties and enhancements (by Lucas & Saccucci). *Technometrics*. 1990;32(1):23-26. https://doi.org/10.2307/1269840
10. Knoth S. *spc: Statistical Process Control —Collection of Some Useful Functions. R package version 0.6.7*. R Foundation for Statistical Computing; 2022.
11. Hawkins DM, Olwell DH. *Cumulative Sum Charts and Charting for Quality Improvement*. Springer-Verlag; 1998.
12. Pollak M, Siegmund D. Approximations to the expected sample size of certain sequential tests. *Ann Stat*. 1975;3(6):1267-1282. https://doi.org/10.1214/aos/1176343284
13. Taylor HM. The economic design of cumulative sum control charts. *Technometrics*. 1968;10(3):479-488. https://doi.org/10.1080/00401706.1968.10490595
14. Woodall WH, Faltin FW. Rethinking control chart design and evaluation. *Qual Eng*. 2019;31(4):596-605. https://doi.org/10.1080/08982112.2019.1582779
15. Capizzi G, Masarotto G. Evaluation of the run-length distribution for a combined Shewhart-EWMA control chart. *Stat Comput*. 2010;20(1):23-33. https://doi.org/10.1007/s11222-008-9113-8

AUTHOR BIOGRAPHY

Sven Knoth is a Professor of Statistics in the Department of Mathematics and Statistics within the School of Economic and Social Sciences at the Helmut Schmidt University, Hamburg, Germany. Prior to that, he worked as a Senior SPC Engineer at Advanced Mask Technology Center (AMTC) Dresden, Germany, from 2004 to 2009. He is an Associate Editor of Computational Statistics, and member of the Editorial Review Boards of Quality Engineering and Journal of Quality Technology.

SUPPORTING INFORMATION

Additional supporting information can be found online in the Supporting Information section at the end of this article.

How to cite this article: Knoth S. Another objection to the homogeneously weighted moving average control chart. *Qual Reliab Eng Int*. 2023;39:353–362. https://doi.org/10.1002/qre.3242